nature materials

ARTICLES

PUBLISHED ONLINE: 5 DECEMBER 2016 | DOI: 10.1038/NMAT4811

Topologically protected bound states in photonic parity–time-symmetric crystals

S. Weimann[1†], M. Kremer[1†], Y. Plotnik[2], Y. Lumer[2], S. Nolte[1], K. G. Makris[3,4], M. Segev[2], M. C. Rechtsman[5] and A. Szameit[1*]

Parity–time (PT)-symmetric crystals are a class of non-Hermitian systems that allow, for example, the existence of modes with real propagation constants, for self-orthogonality of propagating modes, and for uni-directional invisibility at defects. Photonic PT-symmetric systems that also support topological states could be useful for shaping and routing light waves. However, it is currently debated whether topological interface states can exist at all in PT-symmetric systems. Here, we show theoretically and demonstrate experimentally the existence of such states: states that are localized at the interface between two topologically distinct PT-symmetric photonic lattices. We find analytical closed form solutions of topological PT-symmetric interface states, and observe them through fluorescence microscopy in a passive PT-symmetric dimerized photonic lattice. Our results are relevant towards approaches to localize light on the interface between non-Hermitian crystals.

Topological insulators (TIs) are materials that exhibit exceptionally robust transport, potentially enabling applications such as robust spintronic devices and the protection of quantum bits from decoherence[1]. Perhaps the most salient feature of topological systems is the presence of localized states residing at the interface between a TI and its non-topological environment: these surface or edge states are the channels through which robust transport occurs (while in the TI there is no bulk transport due to the band gap). In condensed matter physics, topological systems such as the quantum Hall effect and the quantum spin Hall effect have been extensively studied[1]. Subsequently, the concept of topological physics was introduced to the domain of electromagnetic waves[2,3] through microwave experiments in gyro-optic media[4]. The search for an optical realization of TIs has prompted a number of proposals[5–8], and finally experimental realizations[9–11]. This launched the field of topological photonics[12]—an ongoing research effort to realize the robustness associated with topological electronic transport in photonic systems. Such photonic topological insulators enable direct experimental studies of fundamental concepts in ways that in many cases are extremely hard to implement in condensed matter systems. For example, the concept of Floquet topological insulators[13–15] was first demonstrated in optics[9] and only later observed in ultracold fermions[16] and with electrons in condensed matter systems[17]. The observation of the photonic TI prompted the study of nonlinear waves in TIs and the prediction of topological gap solitons[18], which are now being sought in photonic media and in cold atoms. Moreover, rigorous mathematical approaches for finding topological edge states are now starting to be explored[19]. Equally important, photonic TIs can, in principle, enable robust photonic devices such as waveguides, interconnects, delay lines, isolators and couplers (or anything susceptible to parasitic scattering by fabrication disorder).

In parallel to the progress on photonic topological insulators, there has been a great deal of recent research into non-hermitian optical systems. The origin of this was the observation by Bender and Boettcher[20] that certain non-hermitian Hamiltonians may contain only real eigenvalues provided that they commute with the parity–time (PT) operator. In fact, if the Hamiltonian commutes with the PT operator, then having a real spectrum is equivalent to all eigenstates being eigenstates of the PT operator, or calling the system PT-symmetric. In a series of papers[21,22] this concept was brought into optics by proposing PT-invariant Hamiltonians could be realized by using optical gain and loss. In addition, these optical systems exhibit a unique point in parameter space, the so-called exceptional point[23], where the underlying modes coalesce to a single mode which is orthogonal to itself. Subsequent observations[24–26] have experimentally demonstrated non-hermitian optical systems along with the exceptional points associated with them. Since then, numerous ideas and applications have been proposed, such as PT-based lasers that remain single mode even high above the threshold[27,28], optical isolators[29], and more.

The progress with these two separate topics of photonic topological insulators and PT-optics raises the question whether it is possible to have a topological interface state in a PT-symmetric system. This has been a topic of ongoing discussion, with compelling arguments stating that the realization of a topological interface state in a PT-symmetric system is impossible[30]. One argument saying that this is impossible runs as follows: consider a topological edge state in a one-, two-, or three-dimensional system whose Hamiltonian commutes with the PT operator. Since the action of the PT operator sends this state to the other edge of the system, the state cannot be an eigenstate of PT, and thus necessarily breaks PT symmetry—that is, has a complex eigenvalue. Indeed, in a recent realization, while demonstrating the topological nature of the edge states in a non-hermitian dimer potential, the PT symmetry was broken[31,32]. However, there exist theoretical proposals[33–35] showing that the argument given above can be circumvented and

[1]Institut für Angewandte Physik, Abbe School of Photonics, Friedrich-Schiller-Universität Jena, Max-Wien Platz 1, 07743 Jena, Germany. [2]Physics Department and Solid State Institute, Technion-Israel Institute of Technology, Haifa 32000, Israel. [3]Crete Center for Quantum Complexity and Nanotechnology, Department of Physics, University of Crete, PO Box 2208, 71003 Heraklion, Greece. [4]Institute for Theoretical Physics, Vienna University of Technology, A-1040 Vienna, Austria, EU. [5]Department of Physics, The Pennsylvania State University, University Park, Pennsylvania 16801, USA. †These authors contributed equally to this work. *e-mail: alexander.szameit@uni-jena.de

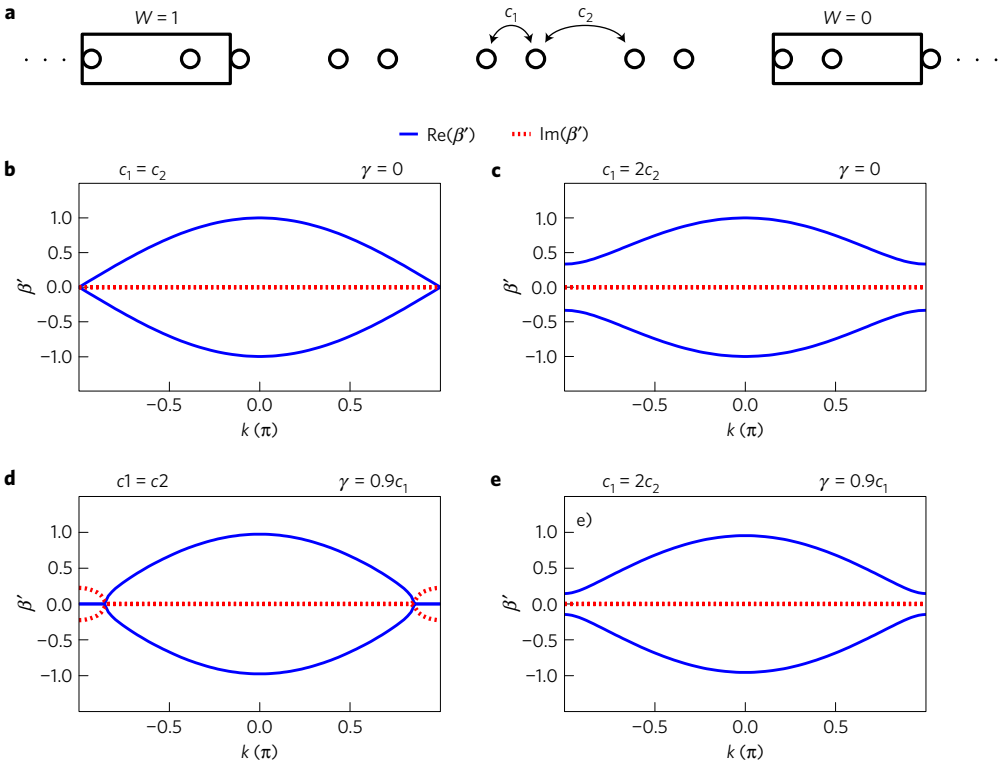

Figure 1 | The infinite dimer lattice and its dispersion relation. a, Sketch of the infinite dimer; the boxes show two topologically distinct configurations of the unit cell. **b**–**e**, Real (solid blue) and imaginary (dotted red) parts of the dispersion relation of the following dimer configurations: lossless and no dimerization (**b**), lossless and dimerized (**c**), alternating gain and loss and no dimerization (**d**), alternating gain and loss and dimerized (**e**). β' is the normalized propagation constant $\beta/(c_1+c_2)$ (following equation (2)). The energy of the topological states arising in the cases **c** and **e** coincide with the imaginary part of the band.

PT-symmetric topological states can indeed be realized. A recent work[36] has studied the dynamics of microwave photons at the interface of PT-symmetric topological lattices. However, the specific realization shown there necessarily gives rise to complex eigenvalues of the interface states and, therefore, this realization does not exhibit global PT symmetry (that is, a purely real eigenvalue spectrum). Another recent work predicts the existence of interface states between regions of broken and unbroken PT symmetry[37]. However, this work did not address topological states in a non-hermitian PT-symmetric system. Namely, the studies by Zhao *et al.* explored only systems where parts of the spectrum were complex. As such, the question about the existence of topological states in systems with PT symmetry still remains open.

Here we propose a simple mechanism for the realization of an optical topological state of full PT symmetry. To realize this, we use an array of evanescently coupled waveguides fabricated using the direct laser writing technique[38]. Below, we first explain our theoretical model, then demonstrate the PT symmetry of the experimental system, and then present the observation of the interface state.

The non-hermitian SSH model

Consider the one-dimensional dimer chain illustrated in Fig. 1a—this is the simplest possible model that exhibits topological edge states—and is also known as the Su–Schrieffer–Heeger (SSH) model[39]. The wavefunction in the system obeys the Schrödinger equation and its unit cell consists of two identical potential wells whose modes have evanescent overlap with their neighbours, with the nearest-neighbour coupling terms c_1 (for the short bond) and c_2 (for the long bond). Henceforth, the magnitude of the difference $\delta = |c_1 - c_2|$ is referred to as the dimerization. Consider now the system in which c_1 and c_2 are interchanged. When such a system is infinite, the bulk is invariant under this transformation of the unit cell. However, in a finite lattice, the edges depend on the exact configuration of the unit cell. As is well known in the SSH model[39,40], the configuration having the smaller coupling at the edges must exhibit edge states, whereas the configuration with the larger coupling at the edges does not. In fact, the two configurations are distinguished by the winding number, given by[41]

$$W_{\mathrm{h}} = \frac{i}{\pi}\oint_{\mathrm{BZ}} \mathrm{d}k \langle\psi_m(k)|\frac{\partial}{\partial k}|\psi_m(k)\rangle \qquad (1)$$

where k is the Bloch wavenumber within the first Brillouin zone (BZ) and m indicates the band (here $m = 1, 2$). The states $|\psi_m(k)\rangle$ and $\langle\psi_m(k)|$ are the eigenvectors of the Hamiltonian in k-space and their hermitian conjugates. In hermitian systems, this is precisely the Zak phase divided by π (ref. 42). The winding number W_{h} takes on the value 0 when there are no edge states and 1 when there are (see Fig. 1b and c, respectively). Our aim is to extend the SSH system to be non-hermitian by introducing alternating gain and loss in a PT-invariant fashion. The additional gain–loss distribution in the potential thus has to be an odd function of position around a given origin. The natural way to realize this is to add $\gamma/2$ of gain to one site in the unit cell and $-\gamma/2$ of loss to the other. This translates to an insertion of alternating $i\gamma/2$ and $-i\gamma/2$ on the diagonal of the Hamiltonian, ensuring the commutation with the PT operator. We discuss the topological invariant for the non-hermitian dimer in Supplementary Note 1. The PT symmetry ensures the existence of a generalized integer winding number, W_{nh} (ref. 43).

The dispersion relation (the relation between the propagation constant β and the transverse wavenumber k) of this system is given by

$$\beta^2 = c_1^2 + c_2^2 + 2c_1c_2\cos(k) - \left(\frac{\gamma}{2}\right)^2 \qquad (2)$$

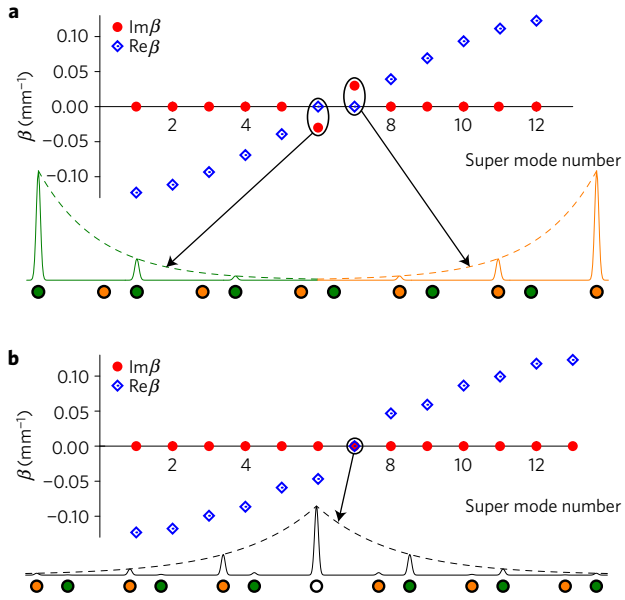

Figure 2 | Spectra of topological interface states in the dimer. a, Sketch of the dimer potential with the two topological edge states. Some of the eigenvalues have positive and negative imaginary parts, as can be seen in the subfigure showing the eigenvalues of the structure (as in ref. 36). **b**, Combination of a non-trivial dimer configuration (centre plus left side) with a trivial configuration of the dimer (right side). The gain–loss profile is globally PT-invariant, the inset shows that the spectrum exhibits entirely real eigenvalues.

Figure 1d shows the two bands of the chain with no dimerization, which are either purely real or purely imaginary, depending on k. The spectrum as a whole indicates broken PT symmetry. As the dimerization is increased, however, the domains of purely imaginary spectrum shrink until $\delta = \gamma/2$ is reached. From this point on, the structure possesses a real spectrum (Fig. 1e), in spite of gain and loss—that is, it is PT-symmetric. In this regime, a band gap opens containing a topological edge state—just like in the lossless case (Fig. 1c).

However, such edge states, either on the sites with gain (orange in Fig. 2a) or on sites with loss (green), must have imaginary eigenvalues[30,36], despite the fact that the PT operator still commutes with the Hamiltonian. Therefore, we must employ another geometry to obtain topological interface states with only real eigenvalues that do preserve the PT symmetry of the entire lattice.

The PT-symmetric topological interface state

Our proposed structure is specifically designed to support PT-symmetric (that is, real-eigenvalued) topological edge states, as shown in Fig. 2b. We terminate the edges at the bond with a large coupling constant on each edge, such that there are no edge states present on either side of the lattice. However, in the centre, we insert a topological defect: instead of the structure having a periodic sequence of dimerized bonds (short-long-short-long-short-long-short), it now has an aperiodic sequence with a double-long defect (short-long-short-long-long-short-long-short). This can be seen as an interface between two structures that have different topological invariants, $W_{\mathrm{nh}} = 0, 1$, and therefore it must possess a topological interface state residing at zero energy at the defect point. We can ensure that $[\mathrm{PT}, H] = 0$ holds true by having neither gain nor loss on the centre point (as shown in Fig. 2b). The parity axis lies at the centre site, and thus the localized interface state does not experience a translation when the PT operator acts on it. As the plot shows, the eigenstate is centred on the central waveguide and indeed exhibits a real eigenvalue. In fact, the whole spectrum has exclusively real eigenvalues, and therefore the system is PT-symmetric, possessing a real winding number. In Supplementary Note 3, we derive the closed form solution of the topological interface state, which reads

$$a_m = \frac{i^{m-n}}{2}\sigma^{|m-n|}\left[A + B + (A-B)(-1)^{m-n}\right] \qquad (3)$$

where a_m is the electric field amplitude in the mth guide and n is the index of the centre site. The quantity A is the amplitude of the state at the central site. The constants B and σ are functions of the loss $\gamma/2$, c_1 and c_2, and are given in Supplementary Note 3. From the symmetries of the SSH lattice, it can be shown that the eigenvalue of the bound solution is completely robust against disorder in the couplings c_1 and c_2. In Supplementary Note 2 we compare profiles of the bound state in a randomized crystal lattice with PT symmetry for different strengths of disorder and prove that the topological state must be real on all sites an even number of waveguides away from the centre one, and imaginary on the others. The disorder we study always preserves the essential symmetries, which are necessary for the existence of a topological bound state.

The realization of the PT-symmetric crystal interface

In the following, we will study the predictions regarding this lattice experimentally using photonic waveguide arrays (see Fig. 3a), which are an exceptional system for implementing PT-symmetric non-hermitian Hamiltonians[21,24,25,31,38,44–47]. In waveguide arrays, an eigenstate is a state that stays invariant as light propagates along the waveguides. Such a state can be either an extended state (a Bloch mode) or a localized state (a defect mode), both being invariant with respect to the evolution coordinate z. As shown previously[46,48], the loss in photonic lattices can be precisely engineered by 'wiggling' the waveguides as a function of z, which causes radiative loss (coupling to the continuum states). The amplitude and frequency of the wiggling can be precisely tuned to achieve a particular loss. Importantly, the non-hermitian PT-symmetric system described above can be mapped directly onto a system with only loss (and no gain) simply by multiplying the wavefunction by an overall decay factor $e^{-\gamma z/2}$, as was demonstrated in refs 24,47. In such 'passive-PT-symmetric' systems, PT-symmetric phenomena can be demonstrated without employing actual gain. The multiplication by a global decay is equivalent to an offset of the imaginary part of the gain–loss profile. For the model shown schematically in Fig. 2b this means that the 'gain' waveguides will be straight (that is, have no loss), the 'lossy' waveguides will exhibit a loss γ, and the central waveguide as well as the surrounding material exhibit a loss $\gamma/2$. Our waveguide arrays are fabricated with the

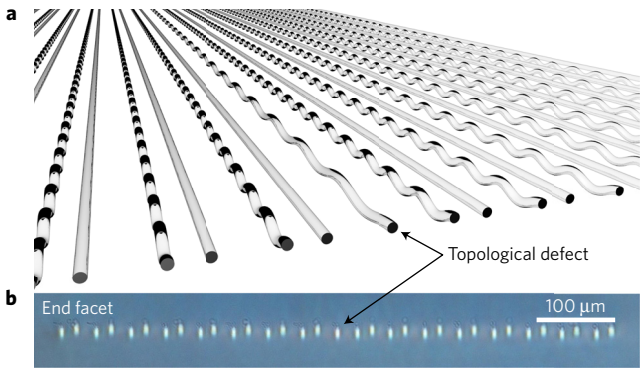

Figure 3 | Realization of the PT-symmetric crystal interface. a, Sketch of the passive waveguide array acting like a PT-symmetric structure with a topological interface. **b**, End facet of the experimentally realized structure in fused silica glass. Image courtesy of Mark Kremer, FSU Jena.

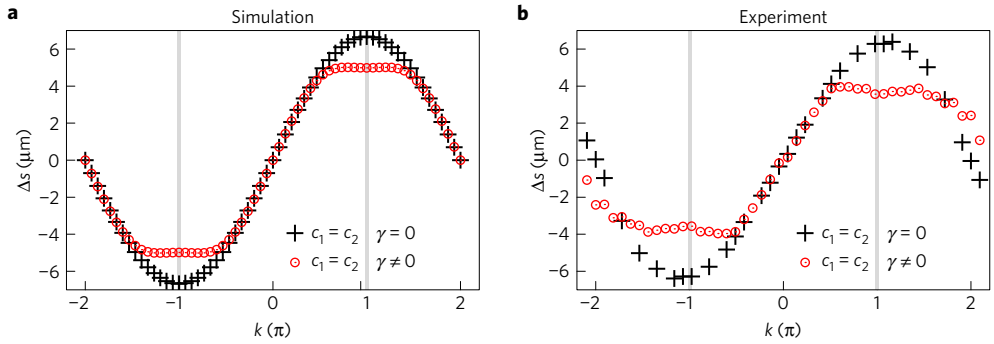

Figure 4 | Translation of the centre of mass (Δs) of a broad Gaussian input beam whose phase front is tilted. a, Simulation of the lossless dimer with (black) and the dimer with alternating gain and loss (red), both with zero dimerization. **b**, Experimentally measured shift in the lossless dimer (black) and in the dimer with alternating gain and loss (red), both with zero dimerization. The lattice parameters are $c_1 = c_2 = 0.08\,\mathrm{mm}^{-1}$, $\gamma = 0.03\,\mathrm{mm}^{-1}$. The grey lines indicate the points $k = \pi$ in the Brillouin zone of the homogeneous, lossless lattice.

femtosecond laser direct writing technique[38]. The inscription of waveguides into nearly lossless fused silica creates the necessity of another approximation, since any difference between losses in the bulk material and losses of the waveguides has been shown to introduce nonzero imaginary parts to the coupling coefficients[24,49]. In the low-loss limit, however, these imaginary parts can be safely neglected.

In the first experiments, we focus on the demonstration of fundamental features of systems whose Hamiltonian commutes with the PT operator but PT symmetry is broken. We start by considering the dimer with alternating loss, but no defect and no dimerization, and compare it to the corresponding Hermitian lattice with no loss. When launching a broad Gaussian beam with a tilted phase front $e^{i\kappa x}$ into the lattices, the slope κ corresponds to the transverse wavenumber k in the Brillouin zone. In hermitian systems κ causes a transverse displacement Δs of the beam's centre of mass while it propagates[50]. Figure 4a,b shows the outcome of simulations and experiments showing the expected shifts Δs in the hermitian (black) and non-hermitian case (red) after a propagation distance of 55 mm. The experimental data are extracted by means of fluorescence microscopy[51]. The cosine-shaped dispersion relation of a simple Hermitian lattice (see Fig. 1b) results in a sine-shaped displacement function $\Delta s(k)$, with two points of maximal displacement at $k = \pm\pi$ (indicated by the grey lines in Fig. 4). These points correspond to the edges of the Brillouin zone in Fig. 1b. However, for the non-hermitian dimer lattice the situation changes. Plateaux in the displacement function appear which are induced by the complex dispersion relation, corresponding to Fig. 1d. This is clearly seen in our experiments and confirmed by the simulations, demonstrating the existence of complex eigenvalues in our lattice.

At this point, it is essential to demonstrate the PT-symmetry-breaking transition as a function of dimerization. We proceed in a manner similar to that in ref. 24, where for a fixed amount of loss, the dimerization of the lattice is driven across the exceptional point. For small or vanishing dimerization, PT symmetry is broken in the lattice, hence the spectrum is complex. Moreover, the light resides predominantly in the waveguides without loss[24]. However, as the dimerization is increased, the system undergoes a transition and PT symmetry is restored, resulting in a real spectrum. Here, the light is essentially equally distributed over sites with and without loss. Hence, looking at the power left after a fixed propagation distance, this power is a decreasing function of the dimerization, following the transition from the regime of broken into unbroken PT symmetry. (Note that we exhibit loss in both broken and unbroken regimes, because we are dealing with a passive PT-symmetric system.) To experimentally demonstrate this feature, we fabricate nine samples with different dimerizations from $\delta = 0\,\mathrm{mm}^{-1}$ to $\delta = 0.1\,\mathrm{mm}^{-1}$, below and above the PT symmetry-breaking point. For reasons

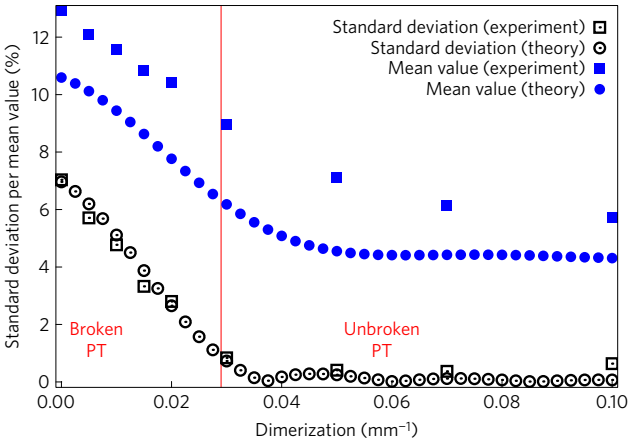

Figure 5 | Loss of guided power in lattices with different dimerizations but fixed loss. Each point summarizes four successive single-waveguide excitations in one waveguide array with a certain dimerization. The average relative power left in the beam after 55 mm propagation is shown in blue, and the standard deviation of the relative power left is shown in black. The lattice parameters are $c_1 = 0.05\,\mathrm{mm}^{-1}$, $\gamma = 0.058\,\mathrm{mm}^{-1}$. The red line indicates the value of $\gamma/2$, the transition point between broken and unbroken PT symmetry.

of simplicity, we fix the coupling constant $c_1 = 0.05\,\mathrm{mm}^{-1}$ and the loss $\gamma = 0.058\,\mathrm{mm}^{-1}$, respectively. In each sample, we perform four single-channel excitations of successive sites and measure (via fluorescence imaging) the power left in the lattice. The extracted data are shown in Fig. 5. As expected, the mean power left in the lattice is monotonically decreasing in both the numerical simulations and experimental data, reaching a minimum when the lattice is in the unbroken phase. (There is an offset of approximately 2% between the experiments and the predictions, associated with the tight-binding calculations. This 2% can be well explained by noise in the fluorescence images after subtraction of the background signal.) In addition, we plot the standard deviation of the data. As in the broken phase, the eigenvalues exhibit different imaginary parts, and the power left in the lattice depends strongly on which waveguides the light is injected into. In contrast, in the unbroken phase, all eigenvalues exhibit the same imaginary part; that is, the power decay in the lattice is less strongly dependent on the excited waveguide. Therefore, by increasing the dimerization above the critical value of $\gamma/2$, the standard deviation of the transmitted power will eventually vanish. This is clearly seen in Fig. 5, proving that with sufficiently strong dimerization our system is indeed in the PT-symmetric phase.

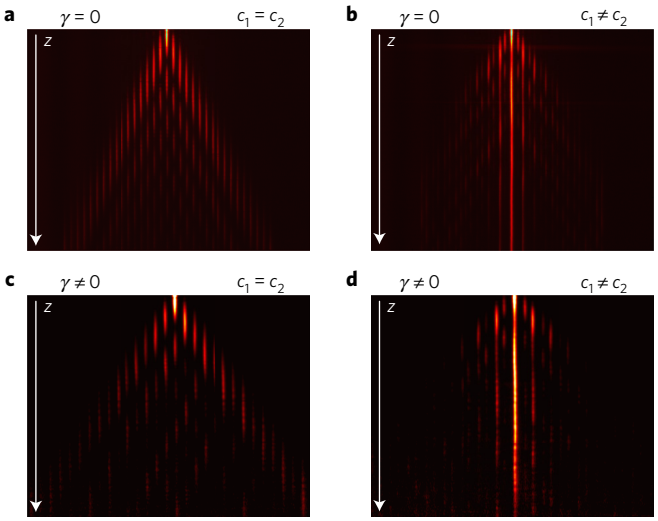

Figure 6 | Fluorescence images of the light evolution after a single-waveguide excitation of the topological defect in different dimer configurations. a, Lossless and vanishing dimerization. **b**, Lossless and dimerized. **c**, Alternating gain and loss and vanishing dimerization. **d**, Alternating gain and loss and dimerized. The lattice parameters are $c_1 = 0.05\,\mathrm{mm}^{-1}$, $\gamma = 0.04\,\mathrm{mm}^{-1}$.

Observation of the topological interface state

In the final experiment, we implement the structure with the defect, as shown in Fig. 3a in the passive-PT framework, and study how the light is trapped at the topological interface for increasing dimerizations passing from broken to unbroken PT symmetry. To this end, we present four fluorescence images of light evolution in arrays that correspond to the scenarios in Fig. 1. Namely, Fig. 6a for the non-dimerized hermitian case, Fig. 6b for the dimerized hermitian case, Fig. 6c for the non-dimerized non-hermitian case (PT-broken), and Fig. 6d for the dimerized non-hermitian case (PT-unbroken). Specifically, Fig. 6a shows the propagation of paraxial light in a non-dimerized array without loss for a single-channel excitation exactly at the central waveguide (where the topological defect is introduced). The wave packet spreads and no trapping is observed, because this system has no interface state at this centre waveguide. The array in Fig. 6b is also lossless, but this time we introduce dimerization of $\delta = 0.12\,\mathrm{mm}^{-1}$ in the unit cell. The interface acts now as a strong defect, with an associated topological state. Consequently, most of the light remains confined to the defect site. In Fig. 6c,d we introduce loss of $\gamma = 0.04\,\mathrm{mm}^{-1}$ in every second waveguide. The loss of the centre site $\gamma/2$ associated with the overall decay is factored out in the image, to allow direct visual comparison with the Hermitian case. In the array without dimerization, Fig. 6c, the PT symmetry is broken, as we proved in the experiment presented in Fig. 5. Here, just as in the lossless case, the beam broadens (no trapping) since there is no defect state. However, when we introduce dimerization of $\delta = 0.12\,\mathrm{mm}^{-1}$ and launch the light directly into the defect, the beam stays confined at the topological interface—as a direct result of the formation of a PT-symmetric topological interface state (Fig. 6d).

In this work, we predicted and experimentally demonstrated a PT-symmetric topological interface state in a non-hermitian system. We derived the state analytically and showed its presence experimentally in a photonic waveguide lattice. We experimentally proved that our system is indeed PT-symmetric, by providing clear evidence for the phase transition from the broken to the unbroken phase. Our results are relevant towards approaches to localize waves at the interface between non-hermitian crystals, but also trigger various questions on the physics of complex non-hermitian crystals.

Data availability. The experimental data that are shown in Figs 4–6 and any related experimental background information not mentioned in the text are available from the authors on request.

Received 3 December 2015; accepted 28 October 2016; published online 5 December 2016

References

1. Hasan, M. Z. & Kane, C. L. Colloqium: topological insulators. *Rev. Mod. Phys.* **82,** 3045–3067 (2010).
2. Haldane, F. D. M. & Raghu, S. Possible realization of directional optical waveguides in photonic crystals with broken time-reversal symmetry. *Phys. Rev. Lett.* **100,** 013904 (2008).
3. Wang, Z., Chong, Y. D., Joannopoulos, J. D. & Soljačić, M. Reflection-free one-way edge modes in a gyromagnetic photonic crystal. *Phys. Rev. Lett.* **100,** 013905 (2008).
4. Wang, Z., Chong, Y. D., Joannopoulos, J. D. & Soljačić, M. Observation of unidirectional backscattering-immune topological electromagnetic states. *Nature* **461,** 772–776 (2009).
5. Umucallar, R. O. & Carusotto, I. Artificial gauge field for photons in coupled cavity arrays. *Phys. Rev. A* **84,** 043804 (2011).
6. Hafezi, M., Demler, E. A., Lukin, M. D. & Taylor, J. M. Robust optical delay lines with topological protection. *Nat. Phys.* **7,** 907–912 (2011).
7. Fang, K., Yu, Z. & Fan, S. Realizing effective magnetic field for photons by controlling the phase of dynamic modulation. *Nat. Photon.* **6,** 782–787 (2012).
8. Khanikaev, A. B. *et al*. Photonic topological insulators. *Nat. Mater.* **12,** 233–239 (2013).
9. Rechtsman, M. C. *et al*. Photonic Floquet topological insulators. *Nature* **496,** 196–200 (2013).
10. Hafezi, M., Mittal, S., Fan, J., Migdall, A. & Taylor, J. M. Imaging topological edge states in silicon photonics. *Nat. Photon.* **7,** 1001–1005 (2013).
11. Cheng, X. *et al*. Robust reconfigurable electromagnetic pathways within a photonic topological insulator. *Nat. Mater.* **15,** 542–548 (2016).
12. Lu, L., Joannopoulos, J. D. & Soljačić, M. Topological photonics. *Nat. Photon.* **8,** 821–829 (2014).
13. Kitagawa, T., Berg, E., Rudner, M. & Demler, E. A. Topological characterization of periodically driven quantum systems. *Phys. Rev. B* **82,** 235114 (2010).
14. Lindner, N. H., Refael, G. & Galitski, V. Floquet topological insulator in semiconductor quantum wells. *Nat. Phys.* **7,** 490–495 (2011).
15. Gu, Z., Fertig, H. A., Arovas, D. P. & Auerbach, A. Floquet spectrum and transport through an irradiated graphene ribbon. *Phys. Rev. Lett.* **107,** 21660 (2011).
16. Jotzu, G. *et al*. Experimental realization of the topological Haldane model with ultracold fermions. *Nature* **515,** 237–240 (2014).
17. Wang, Y. H., Steinberg, H., Jarillo-Herrero, P. & Gedik, N. Observation of Floquet-Bloch states on the surface of a topological insulator. *Science* **342,** 453–457 (2013).
18. Lumer, Y., Plotnik, Y., Rechtsman, M. C. & Segev, M. Self-localized states in photonic topological insulators. *Phys. Rev. Lett.* **111,** 243905 (2013).
19. Fefferman, C. L., Lee-Thorp, J. P. & Weinstein, M. I. Topologically protected states in one-dimensional continuous systems and Dirac points. *Proc. Natl Acad. Sci. USA* **111,** 8759–8763 (2014).
20. Bender, C. M. & Boettcher, S. Real spectra in non-Hermitian Hamiltonians having PT symmetry. *Phys. Rev. Lett.* **80,** 5243 (1998).
21. Makris, K. G., El-Ganainy, R., Christodoulides, D. N. & Musslimani, Z. H. Beam dynamics in PT symmetric optical lattices. *Phys. Rev. Lett.* **100,** 103904 (2008).
22. Musslimani, Z. H., Makris, K. G., El-Ganainy, R. & Christodoulides, D. N. Optical solitons in PT periodic potentials. *Phys. Rev. Lett.* **100,** 030402 (2008).
23. Klaiman, S., Gunther, U. & Moiseyev, N. Visualization of branch points in PT-symmetric waveguides. *Phys. Rev. Lett.* **101,** 080402 (2008).
24. Guo, A. *et al*. Observation of PT-symmetry breaking in complex optical potentials. *Phys. Rev. Lett.* **103,** 093902 (2009).
25. Rüter, C. E. *et al*. Observation of parity–time symmetry in optics. *Nat. Phys.* **6,** 192–195 (2010).
26. Regensburger, A. *et al*. Parity–time synthetic photonic lattices. *Nature* **488,** 167–171 (2012).
27. Hodaei, H., Miri, M.-A., Heinrich, M., Christodoulides, D. N. & Khajavikhan, M. Parity-time-symmetric microring lasers. *Science* **346,** 975–978 (2014).
28. Feng, L., Wong, Z. J., Ma, R.-M., Wang, Y. & Zhang, X. Single-mode laser by parity-time symmetry breaking. *Science* **346,** 972–975 (2014).
29. Nazari, F. *et al*. Optical isolation via PT-symmetric nonlinear Fano resonances. *Opt. Express* **22,** 9574–9584 (2014).

30. Hu, Y. C. & Hughes, T. L. Absence of topological insulator phases in non-Hermitian PT-symmetric Hamiltonians. *Phys. Rev. B* **84,** 153101 (2011).
31. Zeuner, J. M. *et al*. Observation of a topological transition in the bulk of a non-Hermitian system. *Phys. Rev. Lett.* **115,** 040402 (2015).
32. Schomerus, H. Topologically protected midgap states in complex photonic lattices. *Opt. Lett.* **38,** 1912–1914 (2013).
33. Yuce, C. Topological phase in a non-Hermitian PT symmetric system. *Phys. Lett. A* **379,** 1213–1218 (2015).
34. Yuce, C. PT symmetric Floquet topological phase. *Eur. Phys. J. D* **69,** 184 (2015).
35. Harter, A. K., Lee, T. E. & Joglekar, Y. N. PT-breaking threshold in spatially asymmetric Aubry-André and Harper models: hidden symmetry and topological states. *Phys. Rev. A* **93,** 062101 (2016).
36. Poli, C., Bellec, M., Kuhl, U., Mortessagne, F. & Schomerus, H. Selective enhancement of topologically induced interface states in a dielectric resonator chain. *Nat. Commun.* **6,** 6710 (2015).
37. Zhao, H., Longhi, S. & Feng, L. Robust light state by quantum phase transition in non-Hermitian optical materials. *Sci. Rep.* **5,** 17022 (2015).
38. Szameit, A. & Nolte, S. Discrete optics in femtosecond-laser-written photonic structures. *J. Phys. B* **43,** 163001 (2010).
39. Su, W. P., Schrieffer, J. R. & Heeger, A. J. Solitons in polyacetylene. *Phys. Rev. Lett.* **42,** 1698 (1979).
40. Malkova, N., Hromada, I., Wang, X., Bryant, G. & Chen, Z. Observation of optical Shockley-like surface states in photonic superlattices. *Opt. Lett.* **34,** 1633–1635 (2009).
41. Delplace, P., Ullmo, D. & Montambaux, G. Zak phase and the existence of edge states in graphene. *Phys. Rev. B* **84,** 195452 (2011).
42. Zak, J. Berry's phase for energy bands in solids. *Phys. Rev. Lett.* **62,** 2747 (1989).
43. Esaki, K., Sato, M., Hasebe, K. & Kohmoto, M. Edge states and topological phases in non-Hermitian systems. *Phys. Rev. B* **84,** 205128 (2011).
44. El-Ganainy, R., Makris, K. G., Christodoulides, D. N. & Musslimani, Z. H. Theory of coupled optical PT-symmetric structures. *Opt. Lett.* **32,** 2632–2634 (2007).
45. Longhi, S. Optical realization of relativistic non-Hermitian quantum mechanics. *Phys. Rev. Lett.* **105,** 013903 (2010).
46. Eichelkraut, T. *et al*. Mobility transition from ballistic to diffusive transport in non-Hermitian lattices. *Nat. Commun.* **4,** 2533 (2013).
47. Ornigotti, M. & Szameit, A. Quasi PT-symmetry in passive photonic lattices. *J. Opt.* **16,** 065501 (2014).
48. Eichelkraut, T., Weimann, S., Stützer, S., Nolte, S. & Szameit, A. Radiation-loss management in modulated waveguides. *Opt. Lett.* **39,** 6831–6834 (2014).
49. Golshani, M. *et al*. Impact of loss on the wave dynamics in photonic waveguide lattices. *Phys. Rev. Lett.* **113,** 123903 (2014).
50. Eisenberg, H. S., Silberberg, Y., Morandotti, R. & Aitchison, J. S. Diffraction management. *Phys. Rev. Lett.* **85,** 1863 (2000).
51. Szameit, A. *et al*. Quasi-incoherent propagation in waveguide arrays. *Appl. Phys. Lett.* **90,** 241113 (2007).

Acknowledgements

The authors gratefully acknowledge financial support from the Deutsche Forschungsgemeinschaft (grants SZ 276/7-1, SZ 276/9-1, NO462/6-1, BL 574/13-1, GRK 2101/1) and the German Ministry for Science and Education (grant 03Z1HN31). K.G.M. is supported by the People Programme (Marie Curie Actions) of the European Union's Seventh Framework Programme (FP7/2007-2013) under REA grant agreement number PIOF-GA-2011- 303228 (project NOLACOME), and by the European Union Seventh Framework Programme (FP7-REGPOT-2012-2013-1) under grant agreement 316165. M.C.R. acknowledges suport from the Alfred P. Sloan Foundation, the National Science Foundation under grant number ECCS-1509546, as well as the Penn State MRSEC, Center for Nanoscale Science, under the award NSF DMR-1420620. The authors acknowledge useful discussions with D. Leykam, Y. Chong, T. Hughes and H. Schomerus.

Author contributions

S.W. and M.K. did the experimental work and data analysis. S.W., M.K., Y.P., Y.L., K.G.M. and M.C.R. did the theoretical work. K.G.M., M.S., M.C.R., A.S. and S.W. were responsible for the project planning. All authors contributed equally to the manuscript writing.

Additional information

Supplementary information is available in the online version of the paper. Reprints and permissions information is available online at www.nature.com/reprints. Correspondence and requests for materials should be addressed to A.S.

Competing financial interests

The authors declare no competing financial interests.